Regularized inversion method for retrieval of aerosol particle size distribution function in $W^{1,2}$ space

Yanfei Wang, Shufang Fan, Xue Feng, Guangjian Yan, and Yanning Guan

A determination of the aerosol particle size distribution function by using the particle spectrum extinction equation is an ill-posed integral equation of the first kind. To overcome this, we must incorporate regularization techniques. Most of the literature focuses on the Phillips–Twomey regularization or its variations. However, there are drawbacks for some applications in which the real aerosol distributions have large oscillations in a Junge-type distribution. The reason for this is that the scale matrix based on the norm of the second differences in the Phillips–Twomey regularization is too ill-conditioned to filter the large perturbations induced by the small algebraic spectrum of the kernel matrix and the additive noise. Therefore we reexamine the aerosol particle size distribution function retrieval problem and solve it in $W^{1,2}$ space. This setting is based on Sobolev's embedding theorem in which the approximate solution best simulates the true particle size distribution functions. For choosing the regularization parameters, we also develop an *a posteriori* parameter choice method, which is based on the discrepancy principle. Our numerical results are based on the remote sensing data measured by the CE318 sunphotometer in Jia Xiang County, Shan Dong Province, China, and are performed to show the feasibility of the proposed algorithms. © 2006 Optical Society of America

OCIS codes: 010.1100, 010.1110, 280.1100, 100.0100, 100.3190, 000.4430.

1. Introduction

An atmospheric aerosol is a suspension of small solid or liquid particles in the atmosphere, which plays an important role in atmospheric and environmental research since it takes part in many physical and chemical processes in the atmosphere. Because of the wide variety of sources, the properties of atmospheric aerosol particles, such as size, shape, chemical composition, and optical thickness, may be heterogeneous, and their temporal and spatial variation can be very large.[1–3] The aerosol particles are closely related to the aerosol optical properties, especially in urbanized and industrialized areas.[4] A thorough understanding and explanation of the impact of atmospheric aerosol on sunlight transmission in the atmosphere requires a knowledge of aerosol optical properties such as extinction, scattering cross section, phase function, and single-scattering albedo, as well as microphysical aerosol properties, such as the particle size distribution function and light refraction coefficient.[5,6] Meanwhile, aerosol particle size distribution and aerosol optical thickness are two important properties for characterizing the aerosol particles and the correction of the atmosphere.

A. Brief History of Aerosol Particle Size Distribution Function Retrieval

It is well known that the characteristics of aerosol particle size, which can be represented as a size distribution function in the mathematical formalism, say $n(r)$, play an important role in affecting the climate, so it is necessary to determine the size distribution function of the aerosol particles. Since the relationship between the size of atmospheric aerosol particles and the wavelength dependence of the extinction coefficient was first suggested by Angström in 1929, the size distribution began to be retrieved by extinction measurements. First, Angström inferred that the parameters of a Junge size distribution could be obtained by the aerosol optical thickness at multiple wavelengths and produced the useful Angström empirical formula of Junge size distribution $\tau_{aero} = \beta \lambda^{-\alpha}$, in which τ_{aero} is the aerosol optical thickness (AOT), β is the turbidity

Y. Wang (yfwang_ucf@yahoo.com) and Y. Guan are with the State Key Laboratory of Remote Sensing Science, P.O. Box 9718, Beijing 100101, China. S. Fan, X. Feng, and G. Yan are with the Beijing Normal University, Beijing 100875, China. S. Fan is with the Department of Mathematics; X. Feng and G. Yan are with the School of Geography.

coefficient, and α is the Angström exponent reflecting the aerosol size distribution.

The well-known relationship between the aerosol size distribution and AOT τ_{aero} can be written as

$$\tau_{\text{aero}}(\lambda) = \int_0^\infty \int_0^\infty \pi r^2 Q_{\text{ext}}(r, \lambda, \eta) n(r, z) \mathrm{d}z \mathrm{d}r, \quad (1)$$

where r is the particle radius, $n(r, z)$ is the aerosol number density at height z, η is the complex refractive index of the aerosol particles, λ is the wavelength, and $Q_{\text{ext}}(r, \lambda, \eta)$ is the extinction efficiency factor from Mie theory. Performing the height integration, Eq. (1) can be written as

$$\tau_{\text{aero}}(\lambda) = \int_0^\infty \pi r^2 Q_{\text{ext}}(r, \lambda, \eta) n(r) \mathrm{d}r, \quad (2)$$

where $n(r)$ is the columnar aerosol size distribution (i.e., the number of particles per unit of area per the unit radius interval in a vertical column through the atmosphere). Since the AOT can be obtained from the measurements of the solar flux density with sunphotometers, one can retrieve the size distribution by the inversion of AOT measurements through the above equations. This type of method is called extinction spectrometry, which is not only the earliest method to apply remote sensing to determine atmospheric aerosol size characteristics, but also the most mature method thus far.

Phillips[7] and Twomey[8] referred to the above problem to solve the first kind of Fredholm integral equation theoretically, and developed some corresponding linear inversion techniques. Note that $n(r)$ cannot be written analytically as a function of the τ_{aero} values, and a numerical approach must be followed. So far, linear and nonlinear iterative techniques have been developed to solve the Fredholm integral equation. Yamamoto and Tanaka[9] were the first to apply a numerical inversion algorithm to this problem. Grassl[10] presented a new and reliable iterative method to invert the spectral extinction data and obtained the size distributions.[10] Twomey[11] drew a comparison between the constrained linear inversion and an iterative nonlinear algorithm applied to retrieve the aerosol particle size distributions. In both cases, he obtained the aerosol size distribution $n(x)$ from a set of measurements $\{o_i\}$ $(i = 1, \ldots, m)$, where

$$o_i = \int_a^b K_i(x) n(x) \mathrm{d}x + \epsilon_i \quad (x = \ln r), \quad (3)$$

where $K_i(x)$ is the kernel function that could be obtained by the filter transmissions at various air flows. For the constrained linear inversion, Twomey numerically introduced the simple measure of smoothness, the variance of $\vec{n}$ [i.e., $\sum(\vec{n}_j - \vec{n}_{j-1})^2$], which could be written as $\vec{n}^T H \vec{n}$, and referred to the above problem to

solve the vector $\vec{n}$, such that $\vec{n}^T H \vec{n}$ approached a minimum while $\sum \epsilon_i^2$ was held fixed and was solved by the method of Lagrangian multipliers. The results were so disappointing in that this linear method was only successful for reasonable distributions other than the real aerosol distributions in which large oscillations appeared in the Junge-type distribution. In addition, it was restricted to the wide dynamic range of measurements. Aiming to solve this and based on existing iterative methods, a modification was suggested as follows:

$$\vec{n}_p{}^{(i)}(x) = \left[1 + \left[r_p{}^{(i-1)} - 1\right] K_i(x)\right] \vec{n}_p{}^{(i-1)}(x), \quad (4)$$

where

$$r_p{}^{(i-1)} = \frac{o_i}{\int K_i(x) \vec{n}_p{}^{(i-1)}(x) \mathrm{d}x} = \frac{\int K_i(x) n(x) \mathrm{d}x}{\int K_i(x) \vec{n}_p{}^{(i-1)}(x) \mathrm{d}x}.$$

The results showed that this iterative nonlinear algorithm had advantages when the object function and the measurements extended over a wide dynamic range. Furthermore it was more reliable since a smooth initial guess was multiplied by smooth adjusting functions at each step. However, the method was slower than the constrained linear inversion.

King et al.[12] derived an inversion formula that included the magnitudes of the measurement variances and inferred the columnar aerosol size distributions by inversion of spectral optical measurements in Tucson with a solar radiometer. King et al.[12] separated the size of the distribution function into two parts, one of which was a rapidly varying function, while the other was a slowly varying one. By following the method suggested by Phillips[7] and Twomey[8], King et al.[12] concluded that the columnar aerosol size distributions could be classified in terms of three different types of distribution: type I was a Junge distribution, type II was a relatively monodispersed distribution of the lognormal or a gamma distribution, and type III was a two-component system of a Junge distribution plus a relatively monodispersed distribution. They also presented the results of a representative selection together with a discussion of the sensitivity of spectral extinction measurements to the radius limits and refractive index assumed in the inversion. Moreover, the King et al.[12] results were in agreement with those of Curcio.[13] By applying the constrained linear inversion methods,[11] Shaw[14] combined the scattering and extinction matrix into a single matrix to recover the aerosol size spectra.

Nguyen and Cox[15] proposed a modified deconvolution algorithm for inverting the extinction measurements at multiple wavelengths to retrieve particle concentrations and size distributions by solving the previously described Fredholm integral

equation. Ramachandran and Leith[16] modified the algorithm by adding an optimization routine that changed the values of the limits of integration until the standard deviation of the differences between the actual measurements and the back-calculated measurements was minimized. Then they reconstructed the concentrations and size distributions for simulated and experimental measurements of light extinction caused by different aerosols and evaluated its performance.[16] The results showed that the inversion worked well only for aerosols in the accumulation mode (300 nm $< d_{50} <$ 2500 nm, where d_{50} was the count median diameter). This algorithm was reliable for reconstructing multimodal distributions in the accumulation region. However, the reconstructions were of poor quality when the function to be retrieved was the sum of two delta functions. In addition, there was a broadening of the true distributions in the reconstructed frequency distributions. In a subsequent paper Ramachandran and Leith[17] used an iterative tomographic reconstruction algorithm together with the algorithm in Ref. 16 to obtain the spatial distribution of aerosol extinction coefficients and the aerosol size distributions at selected locations. However, their study was based on the assumption that the refractive index was the same between all the aerosol sources. If the sources have different but known refractive indices, any one assumed value would result in errors in reconstruction. So this area needs further research. Additionally, Lumme and Rahola[18] applied a new iterative method, the quasi-minimal residual algorithm (QMR), to the system of linear equations arising in discrete-dispole approximation (DDA) applications. Heintzenberg[19] presented the properties of the lognormal aerosol particle size distribution and the relationships between the integrals of the different moments of the lognormal distribution. Shifrin and Zolotov[20] studied the marine aerosol size distribution by using the concept of regularization. Ye et al.[21] developed a stochastic inverse technique based on a genetic algorithm (GA) to invert particle-size distribution from angular light-scattering data. Bockmann[22] developed a hybrid regularization method for the ill-posed inversion of multiwavelength lidar data in the retrieval of aerosol size distributions. This inverse technique is independent of any given a priori information of particle-size distribution. However, since this method involves solving nonlinear ill-posed equations and singular value decomposition, the cost of computation should be a large burden. Recently, along with the applications of the MODIS remote sensing and the lidar technique, great progress has been made in the retrieval of the aerosol size distribution.[23,24]

B. Brief Review on Measuring Aerosol Particles

For the measuring of aerosol particles, the majority of results of the research on aerosol size distributions have been obtained statistically from direct measurements with instruments called aerosol spectrometers, where different instruments possess different principles. The measurement systems consist mainly of cascade impactors [e.g., a compact multistage cascade impactor (CCI),[25] or an Anderson cascade sampler[26,27]], a diffusion battery (e.g., screen diffusion battery[28,29]), electrical systems [e.g., differential mobility analyzer (DMA)[30]], and optical systems [e.g., an optical particle counter (OPC),[31,32] lidar,[22,33] and the sunphotometer[34]]. Further aspects of aerosol particle size distribution measurements and the physical background of measurement instruments can be found in Refs. 35–37 and the references therein. Our research relies on the optical system sunphotometer CE318, a description of which will be given in Section 2. Even though several applications of the inversion methods for size distributions through optical systems were studied, the methods involved were still the ones that Phillips and Twomey proposed. Moreover, most of the above work was done under the conditions of certain assumed distributions, such as a Junge-type distribution or normal distribution.

As noted above, the traditional Phillips–Twomey method for linear methods was successful only for reasonable distributions other than the real aerosol distributions in which large oscillations appeared in the Junge-type distribution. Overcoming the large oscillations is a major task in retrieval of the aerosol particle size distribution function. Here we study what is believed to be a new solution for the retrieval of aerosol particle size distribution by using field-based measurements with the sunphotometer CE318, which was designed by CIMEL, France. We first formulated the problem in the abstract functional space, then by using Sobolev's embedding theorem, we studied the solution of the problem in $W^{1,2}$ space, which is known as the Tikhonov regularization. Finally, numerical experiments were performed to show the efficiency of the proposed solution.

Section 2 introduces the experimental site in this study and the sunphotometer specifications. Section 3 provides the background for the problem formulation in infinite space and the traditional solution methods. Subsection 3.A formulates the problem by operator equations of the first kind. Subsection 3.B discusses the traditional least-squares error method and states its shortcomings. Subsection 3.C provides a short review of the Phillips–Twomey regularization method. In Subsection 4.A the Tikhonov regularization in $W^{1,2}$ space is presented. In subsection 4.B the numerical implementation from infinite space to finite space is discussed. In Subsection 4.C the aerosol particle size distribution function retrieval problem by the Tikhonov regularization method is addressed, and an a posteriori regularization parameter choice method is introduced. Section 5 uses the ground-based remotely sensed measurements to verify the numerical results. In Section 6 some concluding remarks are given.

2. Experimental Site and Instrument Specifications

Our investigations were carried out in May 2005. The test area in this study was Jia Xiang County, Shan

Dong Province, China. We chose Jia Xiang County as the test area because it is an industrialized area with high pollution, and the environmental status is undergoing control. It is also a typical test region in the China National 863 Project. The county has a great deal of coal mining. The altitude and the pressure of Jia Xiang County are 35–40 m and 1016 hpa, respectively. The relative humidity is 68%; the wind speed in winter is approximately 3.3 m/s, and in summer the wind speed is approximately 3.1 m/s. We performed the data measurement in a region that is located at longitude 116°20′4″ east and latitude 35°17′39″ north of Greenwich. It is approximately 20 km from a small county airport. It is noted that Jia Xiang is not a big city, and there are few incoming airplanes each month. Therefore the traffic may not cause the local air pollution as much as the thermal and humidity regimes in the atmosphere of the measurement area.

The sunphotometer for measuring the attenuation of aerosols is a CE318 (see Fig. 1). The CE318 is manufactured by CIMEL Electronic, Paris, France. It is a portable automatic tracking radiometer measuring the Sun and sky luminances in eight filters over the visible to near-infrared wavelengths, which are used to retrieve atmospheric parameters, including spectral AOT, precipitable vapor, sky radiance distributions, and the ozone amount. Then the aerosol volume and size distribution can be retrieved by inversion modeling of the spectral AOT.

The CE318 instrument comprises three parts: a sensor head, a control box, and a stepping motor system with double axes. The sensor head has two 33 cm collimators. One of them does not have focusing lenses and is used to measure the direct solar radiation. The other has focusing lenses and is used to measure the sky radiance. The field of view (FOV) of both collimators is 1.2°. Moreover, there is a quadrant detector fitted on the sensor head that is used for fine tuning when the sensor head automatically tracks the Sun. The control box is equipped with two microprocessors, which are used to obtain the data and to control the stepping motor system. The step-

Fig. 1. (Color online) Sunphotometer CE318.

Table 1. Characteristics of CE318

CE318 Channels	Central Wavelength (nm)	Calibration Parameter V_0	Bandwidth (nm)
1	1020	12580.00028	10
3	670	28405.62915	10
4	440	15875.01674	10
6	870	24375.26841	10

ping motor system has two degrees of freedom for the azimuth and altitude measurements and controls the elementary Sun tracking by time equations and makes accurate tracking by the quadrant detector system.

The CE318 has four aerosol channels: 440, 670, 870, and 1020 nm, which can be used for estimating aerosol optical thickness (see Table 1). The bandwidth of the spectral channels is 10 nm. A filter at 936 nm is used for measuring atmospheric water vapor. The CE318 is additionally fitted with three polarized filters at 870 nm. The instrument automatically computes the position of the Sun and tracks its movement, and it is also useful for the atmospheric correction of remote sensing data. The CE318 also includes onboard data storage and data transmission capabilities.

3. Background

The general formulation of inversion schemes using the operator theory in functional space is briefly described and illustrated in finite space.

A. Problem Formulation by Operator Equations of the First Kind

A common feature of all particle size distribution measurement systems is that the relation between noiseless observations and the size distribution function can be expressed as a first-kind Fredholm integral equation[11,38,39]

$$\int_{x_a}^{x_b} k(x, y)n(y)\mathrm{d}y = o(x), \qquad (5)$$

where $[x_a, x_b]$ is the integral interval that characterizes the lower and upper limits of the size range of interests, $o(x)$ is an error-free observation, x is a parameter related to particle size (e.g., $x = \ln r$), and $k(x, y)$ is a weighted function (or more generally, the kernel function) that characterizes the classification, losses, and detection properties of the measurement system.

As a practical matter, the observations are usually contaminated by noise. Hence the relation (5) between the observation o_i and the size distribution $n(x)$ is

$$\int_{x_a}^{x_b} k(x, y)n(y)\mathrm{d}y + e(x) = o(x) + e(x) = \mathrm{d}(x), \quad (6)$$

where e is the unknown observation error. Therefore the inverse problem is to solve a perturbed Fredholm

integral equation of the first kind to get the aerosol particle size distribution $n(x)$.

Let us rewrite Eq. (2) in the form of an abstract operator equation

$$K : F \to O,$$

$$Kn \stackrel{\text{def}}{=} \int_0^\infty k(r, \lambda, \eta) n(r) \mathrm{d}r = \tau_{\text{aero}}, \qquad (7)$$

where $k(r, \lambda, \eta) = \pi r^2 Q_{\text{ex}}(r, \lambda, \eta)$, F denotes the function space of aerosol size distributions, and O denotes the observation space. Both F and O are considered to be the separable Hilbert space. Note that τ_{aero} is the measured term, and it inevitably induces errors e. Hence instead of Eq. (7), we have

$$Kn + e = \tau_{\text{aero}} + e = d. \qquad (8)$$

B. Least-Squares Error Solution Method

Using collocation as described in Subsection 4.B for numerical computation, Eq. (8) can be rewritten in matrix–vector form

$$\mathcal{K}\vec{n} + \vec{e} = \vec{d}, \qquad (9)$$

where $\mathcal{K}$ is the discretization of the continuous operator K, and the arrows on n, e, and d represent the corresponding vectors.

The least-squares solution of Eq. (9) in l_2 space refers to the unconstrained optimization problem

$$\min J^{\text{lse}}[\vec{n}] = \frac{1}{2} \|\vec{d} - \mathcal{K}\vec{n}\|_{l_2}^2. \qquad (10)$$

However, the solution of Eq. (10) should be avoidable. The reason is that the minimization of J^{lse} is equivalent to the so-called normal equation

$$\mathcal{K}^T \mathcal{K} \vec{n} - \mathcal{K}^T \vec{d} = 0. \qquad (11)$$

Note that $\mathcal{K}$ is discrete ill-posed, which means that the ratio of the largest singular value to the smallest singular value of $\mathcal{K}$ will approach infinity for a sufficiently large number of discretizing nodes N. Note that

$$\text{cond}(\mathcal{K}^T \mathcal{K}) \gg \text{cond}(\mathcal{K}),$$

hence, Eq. (11) is more ill-posed. This indicates that the regularization is a must for recovering particle size distribution n.

C. Phillips–Twomey Regularization

Phillips–Twomey regularization is based on solving the discrete operator Eq. (9) with constraints. At this point, they solve the following problem given that

$$\mathcal{K}\vec{n} + \vec{e} = \vec{d},$$
$$\|\vec{e}\| \le \Delta \qquad (12)$$

to vary $\vec{e}$ within the permissible limits so that a minimum is attained by a quadratic form $Q(\vec{n}) = (D\vec{n}, \vec{n})$, where D is a preassigned scale matrix. Note that the minimal value is attained by Q on the boundary, i.e., $\|\vec{e}\| = \Delta$, therefore, one actually solves a constrained optimization problem

$$\min_{\vec{n}} Q(\vec{n}),$$
$$\text{subject to } \|\mathcal{K}\vec{n} - \vec{d}\| = \Delta. \qquad (13)$$

By introducing the Lagrangian multiplier μ, one can minimize the Lagrangian functional

$$L_\mu(\vec{n}) = \frac{1}{2} \|\mathcal{K}\vec{n} - \vec{d}\|^2 + \frac{\mu}{2} Q(\vec{n}), \qquad (14)$$

which leads to the following normalized equation:

$$\mathcal{K}^T \mathcal{K} \vec{n} + \mu D \vec{n} - \mathcal{K}^T \vec{d} = 0. \qquad (15)$$

In the Phillips–Twomey formulation of regularization, the choice of the scale matrix is vital. They chose the form of the matrix D by the norm of the second differences, $\sum_{i=2}^{N-1} (\vec{n}_{i-1} - 2\vec{n}_i + \vec{n}_{i+1})^2$, which corresponds to the following form of matrix D:

$$D = \begin{bmatrix} 1 & -2 & 1 & 0 & 0 & 0 & \cdots & 0 & 0 & 0 & 0 \\ -2 & 5 & -4 & 1 & 0 & 0 & \cdots & 0 & 0 & 0 & 0 \\ 1 & -4 & 6 & -4 & 1 & 0 & \cdots & 0 & 0 & 0 & 0 \\ 0 & 1 & -4 & 6 & -4 & 1 & \cdots & 0 & 0 & 0 & 0 \\ \vdots & \vdots & \ddots & \ddots & \ddots & \ddots & \ddots & \vdots & \vdots & \vdots & \vdots \\ 0 & 0 & 0 & \cdots & 0 & 1 & -4 & 6 & -4 & 1 & 0 \\ 0 & 0 & 0 & \cdots & 0 & 0 & 1 & -4 & 6 & -4 & 1 \\ 0 & 0 & 0 & \cdots & 0 & 0 & 0 & 1 & -4 & 5 & -2 \\ 0 & 0 & 0 & \cdots & 0 & 0 & 0 & 0 & 1 & -2 & 1 \end{bmatrix}.$$

However, matrix D is badly conditioned. For example, with $N = 200$, the largest singular value is 15.99801215000452 by double machine precision. The smallest singular value is $6.495571054857827 \times 10^{-17}$ by double machine precision. This indicates that the condition number of matrix D defined by the ratio of the largest singular value to the smallest singular value equals $2.462910807209186 \times 10^{17}$, which is worse. Hence for small singular values of the discrete kernel matrix $\mathcal{K}$, scale matrix D cannot have them filtered even with the large Lagrangian multiplier μ. This numerical difficulty encourages us to study a more robust scale matrix D, which is formulated in the next section.

4. Regularizing Methods for Retrieving the Aerosol Particle Size Distribution Function

In this section, we briefly review the Tikhonov regularization and discuss the application of the theory

to the aerosol particle size distribution function retrieval problem. We show that the regularization in $W^{1,2}$ has a better performance than the highly cited Phillips–Twomey method.

A. Regularization in $W^{1,2}$ Space

A complete theory for regularization was established by Tikhonov and Arsenin.[40] We will employ this theory for the retrieval of the particle size distribution in $W^{1,2}$ space, since it has been noted that the traditional Phillips–Twomey method for a linear method was successful only for reasonable distributions other than the real aerosol distributions that appeared as large oscillations in the Junge-type distribution.

Suppose that we may conclude from *a priori* considerations that the exact aerosol particle size distribution function $n(r)$ corresponding to τ_{aero} is a smooth function, and we assume that $n(r)$ is continuous on $[a, b]$ and has almost everywhere a derivative that is square integrable on $[a, b]$. By Sobolev's embedding theorem,[40,41] the continuous differentiable function $n(r)$ in $W^{1,2}$ space embeds into integrable continuous function space L_2 automatically. Therefore we can construct a regularizing algorithm that has an approximate solution $n_e^{\alpha(e)}(r) \in W^{1,2}[a, b]$ that converges as $\|e\| \to 0$, to $n_{\mathrm{true}}(r)$ in the norm of space $W^{1,2}[a, b]$. In this setting, we construct the functional

$$J^\alpha[n(r)] = \rho_F[Kn, \tau_{\mathrm{aero}}] + \alpha L(n), \quad (16)$$

where

$$\rho_F[Kn, \tau_{\mathrm{aero}}] = \frac{1}{2}\|k(r, \lambda, \eta)n(r) - \tau_{\mathrm{aero}}(\lambda)\|_{L_2}^2,$$

$$L(n) = \frac{1}{2}\|n(r)\|_{W^{1,2}}^2.$$

The definition of the inner product of the two functions $x(t)$ and $y(t)$ in $W^{1,2}$ space is

$$[x(t), y(t)]w^{1,2} \overset{\mathrm{def}}{=} \int_\Omega \left[x(t)y(t) + \sum_{i=1}^n \frac{\partial x}{\partial t_i}\frac{\partial y}{\partial t_j} \right.$$
$$\left. \times \mathrm{d}t_1\mathrm{d}t_2, \ldots, \mathrm{d}t_n \right], \quad (17)$$

where Ω is the assigned interval of the definition.

Assume that the variation of $n(r)$ is flat near the boundary of the integral interval $[a, b]$. So the derivatives of $n(r)$ are zeros at the boundary of $[a, b]$. Now minimizing $J^\alpha[n(r)]$, we obtain the following integro-differential equation with boundary condition[41]

$$\alpha[n''(r) - n(r)] - \int_a^b \bar{k}(r, \xi, \eta)n(\xi)\mathrm{d}\xi = \overline{\tau_{\mathrm{aero}}}(r), \quad (18)$$

$$n'(a) = 0, \; n'(b) = 0, \quad (19)$$

where

$$\bar{k}(r, \xi, \eta) = \int_a^b k(r, \lambda, \eta)k(\xi, \lambda, \eta)\mathrm{d}\lambda,$$

$$\overline{\tau_{\mathrm{aero}}}(r) = -\int_a^b k(r, \lambda, \eta)\tau_{\mathrm{aero}}(\lambda)\mathrm{d}\lambda.$$

Equations (18) and (19) are the regularized form and can be used for the solution of $n(r)$. Now, the discretization is the remaining task.

B. Discrete Implementation

Note that Eq. (16) is an infinite dimensional problem with only a finite set of observations, so it is improbable to implement such a system by computer to get a continuous expression of the size distribution $n(r)$. By using collocation, the infinite problem can be written in a finite-dimensional form by sampling some grids $\{r_j\}_{j=1}^N$ in the interval of interests $[a, b]$. For example, matrix A of the linear operator approximating the integral operator in Eq. (7) by the trapezoid quadrature rule can be written as

$$A_{ij} = \begin{cases} h_r k(r_i, \lambda_j, \eta), & j = 2, \ldots, N-1 \\ \dfrac{h_r}{2}k(r_i, \lambda_j, \eta), & j = 1, N \end{cases} \quad (20)$$

for different i, where h_r is the step size of the grids in $[a, b]$, which can be equidistant if $h_r = (b - a)/(N - 1)$ or different if h_r is variable or adaptive.

In general, when solving Eq. (16) we always have to keep track of the fact that the error of approximating the integral in Eq. (7) is substantially smaller than the error of specifying the right-hand side. For this reason, it is necessary either to choose sufficiently dense grids, increasing the dimension of the problem, or to use more exact quadrature formulas. However, at the same time, the computing time expenditures and the degree of the underdetermination become higher.

Using the difference scheme

$$r_i = a + (i - 0.5)h_r, \quad i = 1, 2, \ldots, N; \quad h_r = \frac{b-a}{N-1},$$

we have the discrete linear equations

$$\alpha\left[\frac{1}{h_r^2}(n_{i-1} - 2n_i + n_{i+1}) - n_i\right] - \sum_{j=1}^N h_r\bar{k}_{ij}n_j = \overline{\tau_{\mathrm{aero}i}},$$

$$i = 1, 2, \ldots, N-1, \quad (21)$$

$$\frac{n_1 - n_0}{h_r} = 0, \quad \frac{n_{N+1} - n_N}{h_r} = 0, \quad (22)$$

Table 2. Meteorological Data in the Jia Xiang Measurement Area[a]

Date	Time	WFS	HV (km)	T (°C)	RH (%)	LP (hPa)	VP (hPa)	WC
29 April 2005	10:00	3	2.8	25.6	68	998.1	22.4	Thin cloud, smoky
	11:00	3	3	27.4	66	997.7	24.1	
30 April 2005	9:00	3	1.5	24.5	82	995.7	25.2	Thin cloud, PS, foggy and smoky
	10:00	2	1.6	26.4	75	995.5	25.9	
2 May 2005	9:00	2	8	18.9	47	1010.4	10.2	Thin cloud, Smoky at 9:00 to
	10:00	3	8	20.2	31	1010	7.3	11:00, PC from 11:00
	11:00	2	10	21.5	31	1010	8	
	12:00	1	12	22.9	32	1010.1	9	
	13:00	1	12	24.2	29	1009.1	8.7	
	14:00	3	12	24.4	31	1008.1	9.5	
3 May 2005	9:00	3	10	18.7	47	1006.8	10.1	Mostly cloudy, AC
	10:00	4	10	20.7	50	1006.1	12.1	
	11:00	3	12	22.3	50	1005.4	13.1	
	12:00	5	12	23.3	40	1004.6	11.6	
	13:00	5	15	24.9	41	1004.1	13.1	
	14:00	3	18	25.6	33	1003.4	10.9	
6 May 2005	9:00	3	14	17.3	51	1006.9	10.1	Cloudless, sunny
	10:00	1	16	18.2	35	1006.6	7.4	
	11:00	0	20	17.8	32	1006.4	7.4	
7 May 2005	10:00	6	12	20.9	47	996.6	11.6	Mostly cloudy, PS, PC at
	11:00	6	12	22.7	45	996	12.3	10:30–10:45
8 May 2005	9:00	2	10	19.7	26	1005.5	6	Light cloudy
	10:00	2	12	20.9	25	1005.8	6.2	
	11:00	2	15	22.1	22	1005.2	5.8	
	12:00	1	15	24.9	19	1005	6	
	13:00	2	15	24	26	1004.2	7.8	
9 May 2005	9:00	0	10	19.1	54	1003.4	11.9	Cloudless, sunny and smoky
	10:00	0	8	22.4	73	1003.4	19.8	
	11:00	0	8	23	63	1003.3	17.7	
	12:00	0	8	22.4	59	1002	16	
	13:00	1	8	23.9	61	1002.7	18.1	
	14:00	0	7	25.5	56	1002.3	18.3	
11 May 2005	9:00	6	0.9	19.1	84	1001.9	18.6	Foggy at 9:00–10:00, smoky
	10:00	4	2.3	22.6	67	1002.6	18.4	from 11:00
	11:00	3	6	22.7	52	1003.1	14.3	
	12:00	3	7	23.2	49	1003.5	13.9	

[a]There is no observation data on 1 May, 4 May, 5 May, and 10 May due to bad weather conditions.

where $n_i = n(r_i)$; $\bar{k}_{ij} = \bar{k}(r_i, \xi_j, \eta)$, and $\overline{\tau_{\text{aero}i}} = \overline{\tau_{\text{aero}}}(r_i)$ are defined by

$$\bar{k}(r_i, \xi_j, \eta) = \int_a^b k(r_i, \lambda, \eta)k(\xi_j, \lambda, \eta)d\lambda,$$

$$\overline{\tau_{\text{aero}}}(r_i) = -\int_a^b k(r_i, \lambda, \eta)\tau_{\text{aero}}(\lambda)d\lambda.$$

From Eq. (20) and by denoting $A = (A_{ij})_{N \times N}$, $\vec{n}$ and $\overrightarrow{\tau_{\text{aero}}}$ the corresponding vectors, we have from Eqs. (21) and (22) that

$$A^T A \vec{n} + \alpha H \vec{n} - A^T \overrightarrow{\tau_{\text{aero}}} = 0, \qquad (23)$$

where H is a triangular matrix in the form

$$H = \begin{bmatrix} 1+1/h_r^2 & -1/h_r^2 & 0 & \cdots & 0 \\ -1/h_r^2 & 1+2/h_r^2 & -1/h_r^2 & \cdots & 0 \\ \vdots & \ddots & \ddots & \ddots & \vdots \\ 0 & \cdots & -1/h_r^2 & 1+2/h_r^2 & -1/h_r^2 \\ 0 & \cdots & 0 & -1/h_r^2 & 1+1/h_r^2 \end{bmatrix}.$$

Suppose we are interested in the particle size in the interval [0.1, 4] μm, the step size is $h_r = 3.9/(N - 1)$. Now choosing the discrete nodes $N = 200$, the largest singular value of H is $1.041482176501067 \times 10^4$ by double machine precision, and the smallest singular value of H is 0.99999999999953 by double machine precision. Compared to scale matrix D of the Phillips–Twomey regularization, the condition number of H is $1.041482176501554 \times 10^4$, which is better than D in filtering small singular values of the discrete kernel A.

C. Aerosol Particle Size Distribution Function Retrieval

To retrieve the aerosol particle size distribution function $n(r)$, we need to solve the linear Eq. (23) for the AOT at different wavelengths. We are interested in the particle size in the interval [0.1, 10] µm. Note that a coarse difference gridding ($N \leq 20$) induces large quadrature errors, therefore we chose the large difference gridding size of $N = 200$.

To perform the numerical computations, we apply the technique developed by King $et\ al.$,[12] that is, we assume that the actual aerosol particle size distribution function consists of the multiplication of two functions $h(r)$ and $f(f)$: $n(r) = h(r)f(r)$, where $h(r)$ is a rapidly varying function of r, while $f(r)$ is more slowly varying. In this way we have

$$\tau_{\mathrm{aero}}(\lambda) = \int_a^b [k(r,\ \lambda,\ \eta)h(r)]f(r)\mathrm{d}r, \qquad (24)$$

where $k(r, \lambda, \eta) = \pi r^2 Q_{\mathrm{ex}}(r, \lambda, \eta)$, and we denote $k(r, \lambda, \eta)h(r)$ as the new kernel function corresponding to a new operator Ξ:

$$(\Xi f)(r) = \tau_{\mathrm{aero}}(\lambda). \qquad (25)$$

For simplicity of notation, the discretization of Ξ is again denoted by matrix A.

Note that choosing the regularization parameter α is also a major issue in numerical computation. In theory, α can neither be too large nor too small. A larger α yields a well-posed problem but the solution is far from the true value. On the other hand, a smaller α yields a better approximation but with large instabilities. Therefore a trade-off must be found to balance the ill-posed nature of the discrete matrix A. There are two types of parameter selection method: the $a\ priori$ way and the $a\ posteriori$ way. Practically, for an $a\ priori$ choice of the regularization parameter, α should be limited to within $(0, 1)$. For example, we can set α equal to 0.005 or 0.01. However, an $a\ priori$ choice of regularization parameter α does not have the noise/error involved in consideration. Therefore it is not an optimized one, which means the solution is not an optimized solution. So, we consider the $a\ posteriori$ approach for choosing the regularization parameter.

From Eq. (23) we have the particle size distribution function $\vec{n}(r)$, which is closely related to parameter α. So we denote $\vec{n}_\alpha(r)$ instead of $\vec{n}(r)$ as the retrieved value in the numerical computation. We use the widely cited discrepancy principle to find an optimized regularization parameter α^*,[40,41] which is the root of the nonlinear function

$$\Psi(\alpha) = \|A\vec{n}_\alpha - \overrightarrow{\tau_{\mathrm{aero}}}\|^2 - \delta^2, \qquad (26)$$

where δ is the error level to specify the initial data. It is easy to show that $\Psi(\alpha)$ is differentiable. Therefore

fast algorithms for solving α^* can be implemented such as the cubic convergent algorithm developed in Ref. 42:

$$\alpha_{k+1} = \alpha_k - \frac{2\Psi(\alpha_k)}{\Psi'(\alpha_k) + \left[\Psi'(\alpha_k)^2 - 2\Psi(\alpha_k)\Psi''(\alpha_k)\right]^{1/2}}. \qquad (27)$$

Denoting $\beta(\alpha) = \|H^{1/2}\vec{n}^\alpha\|^2$, we have

$$\Psi'(\alpha) = -\alpha\beta'(\alpha),$$

$$\Psi''(\alpha) = -\beta'(\alpha) - 2\alpha\left[\left\|H^{1/2}\frac{\mathrm{d}\vec{n}_\alpha}{\mathrm{d}\alpha}\right\|^2 + \left(H\vec{n}_\alpha,\ \frac{\mathrm{d}^2\vec{n}_\alpha}{\mathrm{d}\alpha^2}\right)\right],$$

where

$$\beta'(\alpha) = 2\left(H\frac{\mathrm{d}\vec{n}_\alpha}{\mathrm{d}\alpha},\ \vec{n}_\alpha\right).$$

Table 3. Descriptions of the Abbreviations

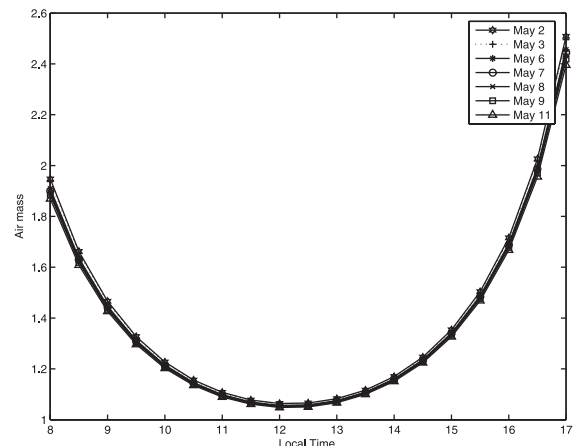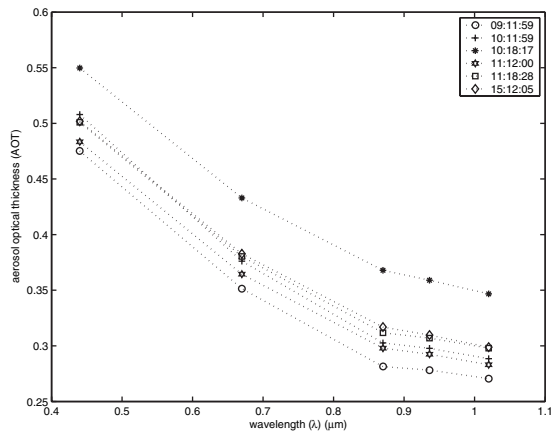| Abbreviations	Descriptions
WC	Weather conditions
HV	Horizontal visibility
VV	Vertical visibility
T	Atmospheric temperature
RH	Relative humidity
LP	Local pressure
VP	Pressure of water vapor
WFS	State of wind force (wind speed)
HVC	High vapor content
LVC	Low vapor content
AC	Altostratus cloud
PS	Partly sunny
PC	Partly cloudy

Fig. 2. Air-mass variation at local time from 2 May to 11 May 2005.

Fig. 3. Variation of AOT on 2 May 2005.

Fig. 5. Variation of AOT on 8 May 2005.

Finding $\vec{n}_\alpha$, $\mathrm{d}\vec{n}_\alpha/\mathrm{d}\alpha$, and $\mathrm{d}^2\vec{n}_\alpha/\mathrm{d}\alpha^2$ will lead to a solution of the following equations:

$$\left(A^T A + \alpha H\right)\vec{n}_{\alpha_k} = A^T \overrightarrow{\tau_{\mathrm{aero}}}, \tag{28}$$

$$\left(A^T A + \alpha H\right)\vec{n}_{\alpha_k}{}' = -H\vec{n}_{\alpha_k}, \tag{29}$$

$$\left(A^T A + \alpha H\right)\vec{n}_{\alpha_k}{}'' = -2H\vec{n}_{\alpha_k}{}'. \tag{30}$$

For the solution of the linear matrix–vector Eqs. (28)–(30), we use the Cholesky decomposition method. A remarkable characteristic of the solution of Eqs. (28)–(30) is that the Cholesky decomposition of the coefficient matrix $A^T A + \alpha H$ needs only once then the three vectors $\vec{n}_\alpha$, $\mathrm{d}\vec{n}_\alpha/\mathrm{d}\alpha$, $\mathrm{d}^2\vec{n}_\alpha/\mathrm{d}\alpha^2$ can be obtained cheaply.

5. Discussion of Numerical Results

Here we choose the ground measured data of sunphotometer CE318 (see Fig. 1) to test the feasibility of the proposed algorithm. We performed successive experiments using the CE318 from 29 April to 11 May 2005 (see Table 2) for meteorological information and weather conditions. To simplify notations, we describe several abbreviations for weather conditions that are used in Table 2. Please refer to Table 3 for the description details.

In these tests, only 2 May, 6 May, 8 May, and 9 May were used for aerosol inversion. Of the days cited, 6 May and 9 May were cloudless and sunny. On May 6 the weather was perfect, sunshine without clouds, with an average wind speed of 1.67 m/s, and a horizontal visibility from 14 to 20 km. On 9 May, there was sunshine but with gray skies and smoke, with an average wind speed of 0.17 m/s and a horizontal visibility from 7 to 10 km. On 2 May, it was smoky and the skies were partly cloudy from 11:00 a.m. with thin clouds. The average wind speed was 2.33 m/s, and the horizontal visibility was 8 to 12 km. On 8 May, the skies were lightly cloudy. The average wind speed was 1.80 m/s and the horizontal visibility was 10 to 15 km. Since sunphotometer CE318 can track the Sun and record the digital numbers (DNs), we also chose the AOTs of the two days but we removed some apparent abnormal values.

The air-mass history from 2 May to 11 May is plotted in Fig. 2. It is illustrated from the figures that the air mass did not change too much at local time on the different days but varied rapidly on each day. We calculated the AOT at different wavelengths λ (μm), by using the data measured on 2 May, 6 May, 8 May,
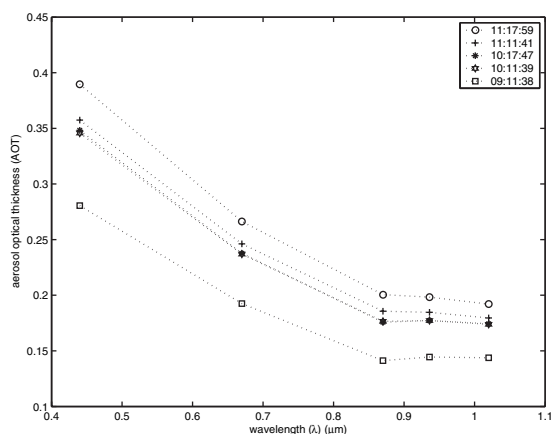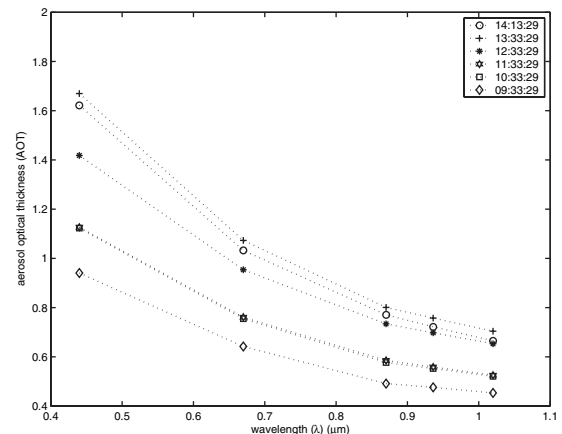

Fig. 4. Variation of AOT on 6 May 2005.

Fig. 6. Variation of AOT on 9 May 2005.

	2 May	6 May	8 May	9 May
α*	2.4909×10^{-6}	1.7281×10^{-6}	1.9998×10^{-6}	5.5219×10^{-6}
	2.6598×10^{-6}	1.6260×10^{-6}	2.9625×10^{-6}	6.2326×10^{-6}
	3.2731×10^{-6}	1.5675×10^{-6}	3.1287×10^{-6}	5.6559×10^{-6}
	2.6221×10^{-6}	1.5686×10^{-6}	3.4677×10^{-6}	4.6148×10^{-6}
	2.7817×10^{-6}	1.2831×10^{-6}	4.1743×10^{-6}	4.6250×10^{-6}
	2.7637×10^{-6}		4.8941×10^{-6}	4.0833×10^{-6}
			4.3825×10^{-6}	
			4.1927×10^{-6}	
	6 measurements	5 measurements	8 measurements	6 measurements

and 9 May. The plots of the AOT variations with regard to wavelength λ on these four days are illustrated in Figs. 3, 4, 5, and 6, respectively. It is obvious from the AOT variation curves of 6 May and 9 May, that the slope of the AOT variation is similar. Evidently, the AOT can change at different times of a day. It increases from morning to noon, approaching its maximum at noon, and decreases with the increase of the wavelength. The magnitudes in both graphs indicate highly polluted air. However, the AOT values on 9 May were larger than those on 6 May. The reason is that the skies on 9 May were smoky, which induced large AOT values, and this coincided with the environmental conditions of Jia Xiang County, according to our measurements. For the AOTs on 2 May and 8 May, because of the effect of the clouds they were not so regular as those on 6 May and 9 May.

We know that Jia Xiang County is an industrialized county with high pollution. The environmental pollution induced by coal and calcareousness mining and also industry combustion has an impact on the air conditions of the local district. Therefore we chose the complex refractive index as η = 1.6−0.1*i*.[26] For the error level δ in specifying the initial data and the approximate degree of quadrature, we chose δ = 0.001, since we chose a large grid number $N = 200$, which sufficiently approximates the integral. In the numerical experiments, we chose the initial guess value α_0 of the regularization parameter as 0.005.

Then each α_k was iteratively calculated by the iteration formula in Eq. (27). The optimum regularization parameters α* for every measurement on each day are recorded in Table 4. It is seen from Table 4 that the optimum values of α* should be approximately $O(1.0e-6)$. By our algorithms, the retrieval results the number of size distribution function $n(r)$ on 2 May, 6 May, 8 May, and 9 May are plotted in Figs. 7–9, and 10, respectively. We see from these figures that there were several rock bottoms in their local neighborhood. On all the chosen days, the particle size distribution function oscillated in the intervals [0.4, 0.7] μm and [7, 10] μm, and changed stably outside these intervals. Even for the data measured on 2 May and 8 May the slope was similar. It can also be seen from the figures that the size distribution for small particles on 9 May is larger than that on other days. This is because on 9 May the air was continuously mixed with smoke, which led to large values of the size distribution function for small particles, whereas for large particles, the size distribution is evidently distinguishable. Since the pollution of Jia Xiang County is mainly the coal combustion type of air pollution, particles of size 0.5 μm constitute the primary particles that can be a major source of air contamination. Large particles of size 7–10 μm are composed mainly of sand, wind, soot, and dust. The results are consistent with the local air conditions and our observations.
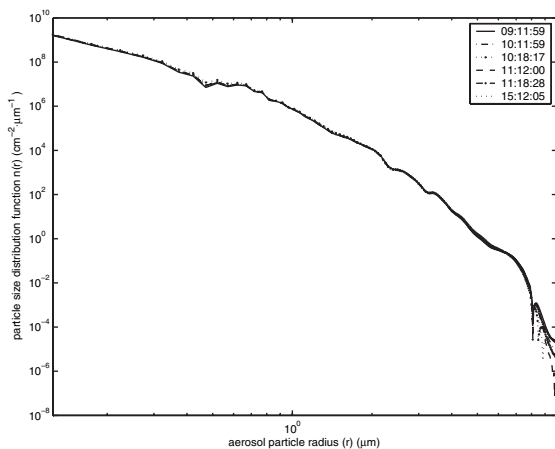

Fig. 7. Particle size distribution on 2 May 2005.
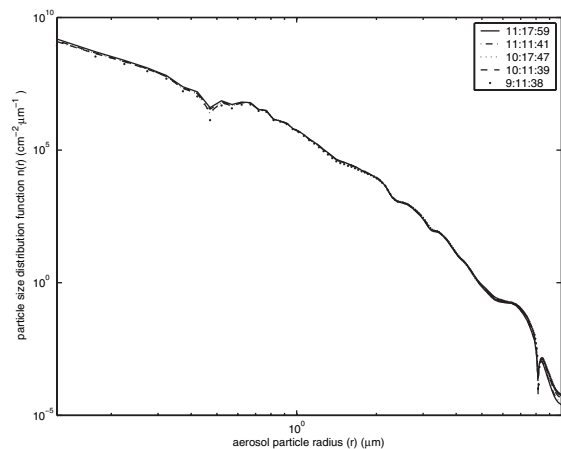

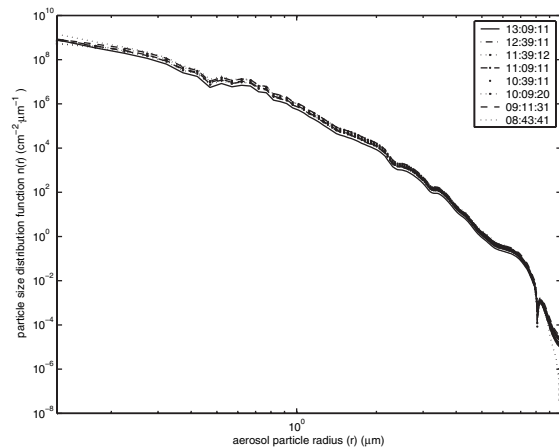Fig. 8. Particle size distribution on 6 May 2005.

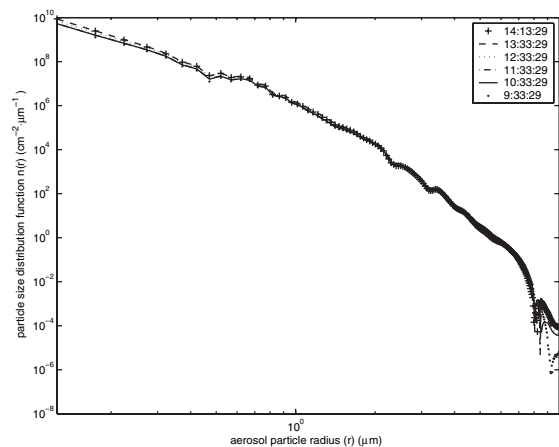Fig. 9. Particle size distribution on 8 May 2005.

Fig. 10. Particle size distribution on 9 May 2005.

6. Concluding Remarks and Future Research

We have investigated the regularization methods for the solution of atmospheric aerosol particle size distribution function retrieval. We reformulated the problem in functional space $W^{1,2}$ by introducing the first-kind Fredholm integral equations. Our method is different from others in the following ways:

(1) Previous research was based mainly on the Phillips–Twomey regularization and its variants. Our approach is based on the Tikhonov regularization in $W^{1,2}$ space.

(2) Previous research on the choice of regularization parameter was *a priori*; that is, the regularization parameter is a preassigned constant. Our approach is *a posteriori*, which is based on the discrepancy, where the regularization parameter approaches an optimum after successive iterations.

(3) A large amount of previous research was based on measurements by optical particle counters, differential mobility analyzers, impactors, diffusion batteries, and lidar. Our research is based on the measurements obtained by using the CE318 sunphotometer, which supplied four aerosol channels that can be best used for estimating aerosol optical thickness.

Hence, it is used for the retrieval of aerosol particle size distribution function $n(r)$.

The numerical experiments illustrate that our new algorithm works well for the retrieval of aerosol particle size distribution functions. Future research will investigate new scale operators D and develop new solution methods, and we will do some numerical verifications based on ground-based remote sensing data and satellite-based remote sensing data in a typical test area of China.

References

1. G. F. Bohren and D. R. Huffman, *Absorption and Scattering of Light by Small Particles* (Wiley, 1983).
2. C. N. Davies, "Size distribution of atmospheric aerosol," J. Aerosol Sci. **5,** 293–300 (1974).
3. S. Twomey, *Atmospheric Aerosols* (Elsevier, 1977).
4. G. J. McCartney, *Optics of the Atmosphere* (Wiley, 1976).
5. A. J. Reagan, D. M. Byrne, D. M. King, J. D. Spinhirne, and B. M. Herman, "Determination of complex refractive index and size distribution of atmospheric particles from bistatic-monostatic Lidar and solar radiometer measurements," J. Geophys. Res. **85,** 1591–1599 (1980).
6. M. Weindisch and W. von Hoyningen-Huen, "Possibility of refractive index determination of atmospheric aerosol particles by ground-based solar extinction and scattering measurements," Atmos. Environ. **28,** 785–792 (1994).
7. D. L. Phillips, "A technique for the numerical solution of certain integral equations of the first kind," J. Assoc. Comput. Mach. **9,** 84–97 (1962).
8. S. Twomey, "On the numerical solution of Fredholm integral equations of the first kind by the inversion of the linear system produced by quadrature," J. Assoc. Comput. Mach. **10** 97–101 (1963).
9. G. Yamamoto and M. Tanaka, "Determination of aerosol size distribution function from spectral attenuation measurements," Appl. Opt. **8,** 447–453 (1969).
10. H. Grassl, "Determinzation of aerosol size distributions from spectral attenuation measurements," Appl. Opt. **10,** 2534–2538 (1971).
11. S. Twomey, "Comparison of constrained linear inversion and an iterative nonlinear algorithm applied to the indirect estimation of particle size distributions," J. Comput. Phys. **18,** 188–200 (1975).
12. M. D. King, D. M. Byrne, B. M. Herman, and J. A. Reagan, "Aerosol size distributions obtained by inversion of spectral optical depth measurements," J. Atmos. Sci. **35,** 2153–2167 (1978).
13. J. A. Curcio, "Evaluation of atmospheric aerosol particle size distribution from scattering measurements in the visible and infrared," J. Opt. Soc. Am. **51,** 548–551 (1961).
14. G. E. Shaw, "Inversion of optical scattering and spectral extinction measurements to receover aerosol size spectra," Appl. Opt. **18,** 988–993 (1979).
15. T. Nguyen and K. Cox, "A method for the determination of

aerosol particle distributions from light extinction data," in *Abstracts of the American Association for Aerosol Research Annual Meeting* (American Association of Aerosol Research, 1989), pp. 330–330.

16. G. Ramachandran and D. Leith, "Extraction of aerosol-size distribution from multispectral light extinction data," Aerosol Sci. Technol. **17,** 303–325 (1992).

17. G. Ramachandran, D. Leith, and L. Todd, "Extraction of spatial aerosol distribution from multispectral light extinction measurements with computed tomography," J. Opt. Soc. Am. A **11,** 144–154 (1994).

18. K. Lumme and J. Rahola, "Light scattering by porous dust particles in the discrete-dipole approximation," Astrophys. J. **425,** 653–667 (1994).

19. J. Heintzenberg, "Properties of lognormal particle size distributions," Aerosol Sci. Technol. **21,** 46–48 (1994).

20. K. S. Shifrin and L. G. Zolotov, "Spectral attenuation and aerosol particle size distribution," Appl. Opt. **35,** 2114–2124 (1996).

21. M. Ye, S. Wang, Y. Lu, T. Hu, Z. Zhu, and Y. Xu, "Inversion of particle-size distribution from angular light-scattering data with genetic algorithms," Appl. Opt. **38,** 2677–2685 (1999).

22. C. Bockmann, "Hybrid regularization method for the ill-posed inversion of multiwave-length lidar data in the retrieval of aerosol size distributions," Appl. Opt. **40,** 1329–1342 (2001).

23. J. T. Mao, C. C. Li, J. H. Zhang, X. Y. Liu, and K. H. L. Alexis, "The comparison of remote sensing aerosol optical depth from MODIS data and ground Sun-photometer observations," J. Appl. Meteorol. Sci. **13,** 127–135 (2002), in Chinese.

24. S. Platnick, M. D. King, S. A. Ackerman, W. P. Menzel, B. A. Baum, J. C. Riédi, and R. A. Frey, "The MODIS cloud products: algorithms and examples from Terra," IEEE Trans. Geosci. Remote Sens. **41,** 459–473 (2003).

25. P. Demokritou, S. J. Lee, S. T. Ferguson, and P. Koutrakis, "A compact multistage (cascade) impactor for the characterization of atmospheric aerosols," J. Aerosol Sci. **35,** 281–299 (2004).

26. J. Liu and C. H. Chen, "A study on remote-sensing inversion of atmospheric aerosol particle size distributions of Lanzhou City in winter," Plateau Meteorol. **23,** 103–109 (2004), in Chinese.

27. B. L. Preidecker, "Bacterial mutagenicity of particulates from Houston air," Environ. Mutagen. **2,** 75–83 (1980).

28. Y. S. Cheng, "Condensation detection and diffusion size separation techniques," in *Aerosol Measurement: Principles, Techniques and Applications,* K. Willeke and P. A. Baron, eds. (Van Nostrand Reinhold, 1993), pp. 427–451.

29. D. Sinclair and G. S. Hoopes, "A novel form of diffusion battery," Am. Ind. Hyg. Assoc. J. **36,** 39–42 (1975).

30. E. O. Knutson and K. T. Whitby, "Aerosol classification by electrical mobility: apparatus, thoery and applications," J. Aerosol Sci. **6,** 453–460 (1975).

31. J. Gebhart, "Optical direct-reading techniques: light intensity systems," in *Aerosol Measurement: Principles, Techniques and Applications,* K. Willeke and P. A. Baron, eds. (Van Nostrand Reinhold, 1993), pp. 313–344.

32. F. Q. Yan, H. L. Hu, and J. Zhou, "Measurements of number density distribution and imaginary part of refractive index of aerosol particles," Acta Opt. Sin. **23,** 854–859 (2003).

33. D. K. Killinger and N. Menyuk, "Laser remote sensing of the atmosphere," Science **235,** 37–45 (1987).

34. G. E. Shaw, "Sun photometry," Bull. Am. Meteorol. Soc. **64,** 4–10 (1983).

35. W. C. Hinds, *Aerosol Technology. Properties Behavior and Measurement of Airborne Particles* (Wiley, 1982).

36. K. Willeke and P. A. Baron eds., *Aerosol Measurement: Principles, Techniques and Applications* (Van Nostrand Reinhold, 1993).

37. P. H. McMurry, "A review of atmospheric aerosol measurements," Atmos. Environ. **34,** 1959–1999 (2000).

38. A. Voutilainenand and J. P. Kaipio, "Statistical inversion of aerosol size distribution data," J. Aerosol Sci. **31** (Suppl. 1), 767–768 (2000).

39. Y. F. Wang, *Computational Methods and Applications for Inverse Problems* (Higher Educational Press, 2006).

40. A. N. Tikhonov and V. Y. Arsenin, *Solutions of Ill-Posed Problems* (Wiley, 1977).

41. T. Y. Xiao, Sh. G. Yu, and Y. F. Wang, *Numerical Methods for the Solution of Inverse Problems* (Science Press, 2003).

42. Y. F. Wang and T. Y. Xiao, "Fast realization algorithms for determining regularization parameters in linear inverse problems," Inverse Probl. **17,** 281–291 (2001).